IOP Publishing Journal of Physics: Condensed Matter
J. Phys.: Condens. Matter **27** (2015) 175008 (16pp) doi:10.1088/0953-8984/27/17/175008

General theory of frictional heating with application to rubber friction

G Fortunato[1], V Ciaravola[1], A Furno[1], B Lorenz[2] and B N J Persson[2]

[1] Bridgestone Technical Center Europe, Via del Fosso del Salceto 13/15, 00128 Rome, Italy
[2] PGI, FZ-Jülich, 52425 Jülich, Germany

E-mail: b.persson@fz-juelich.de

Received 12 January 2015, revised 19 February 2015
Accepted for publication 6 March 2015
Published 15 April 2015

Abstract

The energy dissipation in the contact regions between solids in sliding contact can result in high local temperatures which may strongly effect friction and wear. This is the case for rubber sliding on road surfaces at speeds above 1 mm s^{-1}. We derive equations which describe the frictional heating for solids with arbitrary thermal properties. The theory is applied to rubber friction on road surfaces and we take into account that the frictional energy is partly produced inside the rubber due to the internal friction of rubber and in a thin (nanometer) interfacial layer at the rubber-road contact region. The heat transfer between the rubber and the road surface is described by a heat transfer coefficient which depends on the sliding speed. Numerical results are presented and compared to experimental data. We find that frictional heating results in a kinetic friction force which depends on the orientation of the sliding block, thus violating one of the two basic Leonardo da Vinci 'laws' of friction.

Keywords: contact mechanics, frictional heating, rubber friction

(Some figures may appear in colour only in the online journal)

1. Introduction

When a rectangular block with a nominally smooth surface is squeezed in contact with a nominally flat substrate, because of surface roughness the area of real contact is usually only a very small fraction of the nominal contact area. For hard solids the contact pressure in the area of real contact will therefore be very high. During sliding frictional energy dissipation will take place in the area of real contact and because of the small volumes involved, at high enough sliding speed where thermal diffusion becomes unimportant, the local (flash) temperatures may be very high. As a result local melting of the material, or other phase transformations, can take place. In addition tribochemical reactions and emission of photons or other particles, may occur at or in the vicinity of the contact regions. All these processes will also affect the friction force, e.g. if frictional melting occurs the melted film may act as a lubricant and lower the friction as is the case, e.g. when sliding on ice or snow at high enough velocity. It is clear that a deep understanding of the role of frictional heating is of crucial importance in many cases for understanding friction and wear processes.

Pioneering theoretical works on the temperature distribution in sliding contacts have been presented by Jaeger [1], Archard [2] and others [3–7]. In these studies a moving heat source is located at the sliding interface. However, some materials like rubber have internal friction and when such solids are sliding on a rough surface frictional energy will be dissipated not just at the sliding interface but also some distance into the viscoelastic material. The flash temperature effect related to this process was studied in [8], but neglecting the contribution from the frictional interaction between the surfaces in the area of real contact and also neglecting heat transfer to the substrate. In [9] the theory of [8] was extended to include these effects, but assuming that the substrate has infinite thermal conductivity. In this paper we remove this last restriction and present a general theory of frictional heating.

There are many experimental studies of the temperature in frictional contacts, e.g. see [11]. When analyzing experimental data it is usually assumed that the temperature is continuous at the rubber-substrate interface. However, the latter assumption is in general not valid, in particular if surface roughness exists and the contact area is incomplete within the nominal contact region. One needs to use a heat transfer

description [12–19] which relates the temperature jump $T_R - T_S$ between the rubber surface (T_R) and the substrate surface (T_S) to the heat current J through the interface via $J = \alpha(T_R - T_S)$, where the heat transfer coefficient α in general depends on the sliding speed [9]. We used this more general approach in [9] and also in this paper.

2. Qualitative discussion

Consider a rubber block sliding on a substrate, e.g. a road surface, with random surface roughness. We assume that the substrate can be considered as a rigid material. There will be two contributions to the rubber friction, namely (a) a contribution from the viscoelastic deformations of the rubber which result from the pulsating deformations (frequency ω) it is exposed to from the road asperities and (b) another contribution from the area of real contact. Since most surfaces have roughness on many length scales and since smaller wavelength roughness (wavelength λ) generate higher deformation frequencies $\omega \approx v/\lambda$ (where v is the sliding speed), there will be a wide band of perturbing frequencies usually extending over many frequency decades.

The dissipated frictional energy density, $\dot{Q}(\mathbf{x}, t)$, will be distributed highly non-uniformly in space (and time). In the vicinity of big asperities, the dissipated energy density is small while close to smaller asperities it is higher, and right at the rubber-road interface, in a narrow layer of nanometer thickness, the dissipated energy density (due to the adhesive interaction, process (b)) may be very high. Thus the temperature distribution resulting from the spatial distribution of dissipated energy will, at least for high sliding speeds, be highly non-uniform, changing particularly rapid close to the interfacial contact area. The calculation of the spatial and time dependency of the temperature field is a very complex problem involving solving the heat diffusion equation

$$\left(\frac{\partial}{\partial t} - D\nabla^2\right) T(\mathbf{x}, t) = \frac{\dot{Q}(\mathbf{x}, t)}{\rho C_p}, \qquad (1)$$

where the heat diffusion constant $D = \kappa/\rho C_p$, with a source term $\dot{Q}(\mathbf{x}, t)$ which in general varies rapidly with the spatial and time coordinates over many decades in length and time scales. Clearly, this problem cannot be solved exactly but requires some approximate procedure.

It is usually possible to write the temperature field $T(\mathbf{x}, t)$ as the sum of a slowly varying term $T_0(\mathbf{x}, t)$, plus a fast (in space and time) varying term which we will refer to as the flash temperature. The slowly varying T_0 (background temperature) is, at least in part, the result of the accumulated (or cumulative) effect of the flash temperature. Thus the increase in the background temperature in a tire during breaking is mainly due to the cumulative effect of the flash temperature as the rubber slide over the road surface asperities. For a tire during pure rolling the background temperature is instead mainly due to the energy dissipation in the rubber as a result of compression-decompression of the tread blocks as they pass through the tire-road footprint and due to the flexing of the tire side walls. In both cases the energy dissipated in the rubber will gradually heat up the tire on timescales of order second (during breaking) or longer (during rolling). Both the flash and the background temperature depend in general on external conditions, such as the air and road temperature, or dry or wet condition. However for large slip velocities the flash temperature becomes almost independent of these external conditions. In this paper we will assume that the initial (at time $t = 0$) rubber temperature is constant $T_0(\mathbf{x}, 0) = T_{0R}$, where T_{0R} is independent of the spatial coordinate $\mathbf{x}$. Similarly, we assume that the initial substrate (or road) temperature T_{0S} is constant.

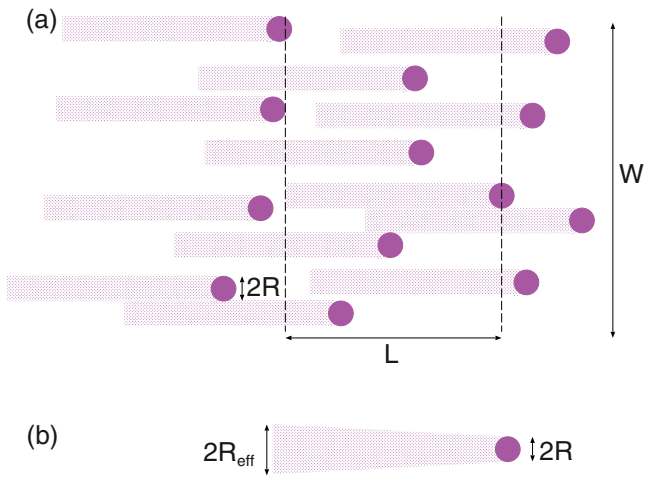

Figure 1. Hot tracks on the rubber surface (dotted area) resulting from the flash-temperature arising in the rubber-road macroasperity contact regions (filled circular regions). (a) shows the hot tracks assuming negligible thermal diffusion and (b) when thermal diffusion is included.

The decomposition of the temperature field into a fast varying flash temperature and a slowly varying background temperature is of course only approximate. In particular, the interaction between hot spots and hot tracks introduce another important (short) time-scale effect usually not considered in analytical studies of the influence of temperature on friction. We illustrate this effect in figure 1(a) where we show the hot tracks on the rubber surface resulting from sliding over road asperities. When the sliding distance is long enough a road asperity—rubber contact area behind another contact region will move into the hot tracks produced by the road asperity—rubber contact regions in front of it. At high enough sliding speed the hot track also gets slightly broadened by heat diffusion (see figure 1(b)). We refer to the interaction between hot spots and hot tracks as a *kinetic thermal interaction*. If l_{av} denotes the average sliding distance needed for a macroasperity contact region to move into the hot track from a macroasperity contact region in front of it, then it takes $\sim t = l_{av}/v$ sliding time before interaction of hot spots becomes important. During this time a hot track has broadened by thermal diffusion by the amount $r \approx (Dt)^{1/2}$. Using $t = l_{av}/v$ this gives $r \approx (Dl_{av}/v)^{1/2}$. Note that $r < l_{av}$ requires $v > v_1 = D/l_{av}$. In a typical case (rubber) $D \approx 10^{-7}\ \mathrm{m^2\ s^{-1}}$ and with $l_{av} \approx 10^{-3}$ m we get $v_1 = 10^{-5}\ \mathrm{m\ s^{-1}}$.

In this study we assume that the rubber surface is smooth and all the roughness exist on the substrate (road) surface. In this case, if a road asperity makes contact with the rubber

block it will stay in contact the whole time from the leading edge of the rubber block to the trailing edge of the block. Thus, the road asperity will continuously heat up and no stationary temperature distribution will develop.

3. Theory

3.1. Basic theory

The following study is based on the rubber friction theory developed in [8, 9, 20]. For a rubber block in dry contact with a hard and rough solid there are two main contributions to rubber friction, namely (a) a contribution derived from the energy dissipation inside the rubber due to the pulsating deformations to which it is exposed to during sliding and (b) a contribution from the shearing processes occurring in the area of real contact. For dry surfaces, the contribution (b) may have different physical origins, e.g. (i) shearing a thin (typically some nm) fluid-like contamination film, or (ii) involving segments of rubber molecules at the rubber surface undergoing binding (to the road surface)–stretching–debonding cycles, or (iii) interfacial crack propagation. Two other contributions to the friction from the area of real contact could result from (iv) rubber wear processes, or (v) the scratching of the hard rubber filler particles (e.g. silica) with the road surface. The contribution from the area of real contact is usually referred to as the adhesive contribution to rubber friction, but this terminology is correct only if the main contribution to the friction from the area of real contact is derived from processes (ii) and (iii). Our present understanding, after analyzing a large set of experimental data is that for asphalt or concrete road surfaces, process (ii) gives the dominant contribution in most cases. The rubber friction experiments of Klüppel *et al* [10] were analyzed assuming that process (iii) dominates.

For sliding at a constant velocity v and neglecting frictional heating, the friction coefficient due to process (a) is:

$$\mu \approx \frac{1}{2}\int_{q_0}^{q_1} \mathrm{d}q\; q^3\, C(q)S(q)P(q) \times \int_0^{2\pi} \mathrm{d}\phi\, \cos\phi\, \mathrm{Im}\frac{E(qv\cos\phi, T_q)}{(1-\nu^2)\sigma_0}, \quad (2)$$

where σ_0 is the nominal contact stress, $C(q)$ the surface roughness power spectrum and $E(\omega, T_q)$ the rubber viscoelastic modulus for the temperature T_q defined below. The friction coefficient depends on the time t via the time-dependency of the velocity v and the temperature T_q.

The function $P(q) = A(\zeta)/A_0$ is the relative contact area when the interface is observed at the magnification $\zeta = q/q_0$, where q_0 is the smallest (relevant) roughness wavevector. We have

$$P(q) = \frac{2}{\pi}\int_0^\infty \mathrm{d}x\; \frac{\sin x}{x}\exp\left[-x^2G(q)\right] = \mathrm{erf}\left(\frac{1}{2\sqrt{G}}\right), \quad (3)$$

where

$$G(q) = \frac{1}{8}\int_{q_0}^{q} \mathrm{d}q\; q^3C(q)\int_0^{2\pi}\mathrm{d}\phi\; \left|\frac{E(qv\cos\phi, T_q)}{(1-\nu^2)\sigma_0}\right|^2. \quad (4)$$

The factor $S(q)$ in (2) is a correction factor which takes into account that the asperity induced deformations of the rubber are smaller than if complete contact would occur in the (apparent) contact areas observed at the magnification $\zeta = q/q_0$. For contact between elastic solids this factor reduces the elastic asperity-induced deformation energy and including this factor gives a distribution of interfacial separation in good agreement with experiments and exact numerical studies [21].

The interfacial separation describes how an elastic (or viscoelastic) solid deforms and penetrates into the roughness valleys and it is these (time-dependent) deformations which cause the viscoelastic contribution to rubber friction. We assume that the same $S(q)$ reduction factor as found for elastic contact is valid also for sliding contact involving viscoelastic solids. For elastic solids $S(q)$ is well approximated by

$$S(q) = \gamma + (1-\gamma)P^2(q), \quad (5)$$

where $\gamma \approx 1/2$. Below we will use the same expression for viscoelastic solids. Note that $S \to 1$ as $P \to 1$ which is an exact result for complete contact. In fact, for complete contact the expression (2) with $S = 1$ is exact.

The second contribution (b) to the rubber friction force, associated with the area of contact observed at the magnification $\zeta_1 = q_1/q_0$, is given by $\tau_f A_1$. Here, $\tau_f(v, T)$ is the (weakly) velocity and temperature-dependent effective frictional shear stress acting in the contact area $A_1 = A(\zeta_1) = P(q_1)A_0$. In this study we consider the flash temperature associated with the viscoelastic contribution and the contribution from the area of real contact to the rubber friction. We note that recently the rubber friction theory presented above (in the absence of the frictional heating, i.e. with $T_q = T_{0\mathrm{R}}$) has been shown to be in good agreement with exact numerical results [22].

Consider a macroasperity contact region which we treat as a circular region with radius R (typically $R \approx 1$ mm). In a macroasperity contact region occur many smaller closely spaced microasperity contact regions. We smear out laterally the frictional energy generated by these microasperity contact regions, which will result in a function $\dot{Q}(z, t)$ describing the dissipated frictional energy per unit time and volume a distance z into the solid in a macroasperity contact region. Let us write

$$\frac{\dot{Q}(z,t)}{\rho C_p} = \int_0^\infty \mathrm{d}q\; f(q,t)\mathrm{e}^{-2qz}. \quad (6)$$

We define the heat flow current

$$J(t) = \int_0^\infty \mathrm{d}z\; \dot{Q}(z,t), \quad (7)$$

and the temperature

$$T_q(t) = \frac{\int_0^\infty \mathrm{d}z\; T(z,t)\mathrm{e}^{-2qz}}{\int_0^\infty \mathrm{d}z\; \mathrm{e}^{-2qz}}. \quad (8)$$

In [8] we have shown that

$$T_q(t) = T_{0\mathrm{R}} + \int_0^t \mathrm{d}t'\; h(w(t,t'))\int_0^\infty \mathrm{d}p\; f(p,t')\frac{1}{\pi} \times \int_0^\infty \mathrm{d}k\; \frac{4q^2}{k^2+4q^2}\frac{4p}{k^2+4p^2}\mathrm{e}^{-Dk^2(t-t')}, \quad (9)$$

where

$$f(p,t) = \frac{v(t)}{\rho C_p} q^4 C(q) S(q) \frac{P(q,t)}{P(q_m,t)} \times \int_0^{2\pi} \mathrm{d}\phi \cos\phi \, \mathrm{Im} \frac{E(qv(t)\cos\phi, T_q(t))}{1-\nu^2}, \quad (10)$$

and

$$h(w) = 1 - \frac{2}{\pi} w(1-w^2)^{1/2} - \frac{2}{\pi} \arcsin(w), \quad (11)$$

where

$$w = w(t,t') = [x(t) - x(t')]/2R,$$

where $x(t)$ is the coordinate of the sliding contact at time t. For uniform sliding speed we have $x(t) = vt$ and $w = (v/2R)(t-t')$. In (10) $P(q_m,t) = A_m(t)/A_0$ is the relative contact area at the magnification $\zeta_m = q_m/q_0$ where the macroasperity contact regions are observed (see [8]).

The integral over k in (9) cannot be solved analytically but in [9] we have shown that

$$T_q(t) \approx T_{0\mathrm{R}} + \int_0^t \mathrm{d}t' \int_0^\infty \mathrm{d}p \; f(p,t') \times \frac{qh(w(t,t'))}{q+p+qp[4\pi D(t-t')]^{1/2}}. \quad (12)$$

We now consider the temperature increase due to the frictional interaction in the area of contact (sometimes denoted as the adhesive rubber-counter surface contribution to the friction). In this case we expect the dissipated frictional energy to be localized in a thin layer of nanometer thickness d at the sliding interface. Thus we take

$$f(q,t) = f(t) q_a \delta(q - q_a), \quad (13)$$

with $q_a \approx 1/d$. This gives

$$\frac{\dot{Q}(z,t)}{\rho C_p} = f(t) q_a \mathrm{e}^{-2q_a z}. \quad (14)$$

From (7) we get

$$f(t) = \frac{2J(t)}{\rho C_p}. \quad (15)$$

Substituting (13) and (14) in (12) gives

$$T_q(t) \approx T_{0\mathrm{R}} + \frac{1}{\rho C_p} \int_0^t \mathrm{d}t' \frac{2qq_a h(w(t,t'))J(t')}{q+q_a+qq_a[4\pi D(t-t')]^{1/2}}. \quad (16)$$

Unless the time t is extremely small, the temperature at the surface is obtained from (16) as

$$T_q(t) \approx T_{0\mathrm{R}} + \frac{1}{\rho C_p} \int_0^t \mathrm{d}t' \frac{2h(w(t,t'))J(t')}{[4\pi D(t-t')]^{1/2}}. \quad (17)$$

In general one expects a temperature jump at the interface between two solids. The heat current through the interface is related to the temperature on the two sides, say the rubber temperature T_R and the substrate (e.g. asphalt road surface) temperature T_S via [12, 13, 19]

$$J_1 = \alpha(T_\mathrm{R} - T_\mathrm{S}), \quad (18)$$

where α is the heat transfer coefficient which in general depends on the sliding speed (see [9]). If the heat current flowing into the substrate is J_1, the heat current into the rubber will be $J_0(t) = J(t) - J_1(t)$.

The substrate temperature in a macroasperity contact region is given by

$$T_\mathrm{S}(t) \approx T_{0\mathrm{S}} + \frac{1}{\rho' C_p'} \int_0^t \mathrm{d}t' \frac{2J_1(t')}{[4\pi D'(t-t')]^{1/2}},$$

or

$$T_\mathrm{S}(t) \approx T_{0\mathrm{S}} + \int_0^t \mathrm{d}t' \frac{g(t')}{[4\pi D'(t-t')]^{1/2}}, \quad (19)$$

where

$$g(t) = \frac{2J_1(t)}{\rho' C_p'}. \quad (20)$$

Here $T_{0\mathrm{R}}$ and $T_{0\mathrm{S}}$ are the rubber and road initial ($t = 0$) temperatures and C_p and C_p' the rubber and road heat capacities. The heat diffusion coefficients D and D' of the rubber and road surfaces are defined by $D = \kappa/\rho C$ and $D' = \kappa'/\rho' C'$, where κ (ρ) and κ' (ρ') are the heat conductivities (mass densities) of the rubber and the road, respectively. If μ_cont is the contribution to the friction coefficient from the area of contact, then

$$J(t) = \mu_\mathrm{cont}(t)\sigma_0 v(t) A_0/A_m,$$

and the equation $J_0 + J_1 = J$ can be written as

$$f(t) + \epsilon g(t) = \frac{2\mu_\mathrm{cont}(t)\sigma_0 v(t)}{\rho C_p} \frac{A_0}{A_m}, \quad (21)$$

where

$$\epsilon = \frac{\rho' C_p'}{\rho C_p}. \quad (22)$$

We now consider sliding at a constant velocity v. Let us assume that the surface temperature on the road asperities in the macroasperity contact region changes slowly with time compared to the time period R/v. This will be the case after a sliding distance $s \gg R$. It also holds for any sliding distance in the limiting case where the thermal conductivity of the substrate (road) surface is infinitely high (see [9]). In the latter case the temperature in the substrate will be $T_{0\mathrm{S}}$ everywhere and in particular $T_\mathrm{S} = T_{0\mathrm{S}}$.

When the surface temperature on the road asperities in the macroasperity contact region changes slowly with time we can treat $T_S(t)$ as a constant during the time period from t to $t+\tau$ where $\tau = 2R/v$. Thus the quantities $f(p,t)$ and $f(t)$ can be treated as (approximately) time independent during the time interval from t to $t+\tau$. We have

$$J_0 = J - J_1 = J - \alpha(T_\mathrm{R} - T_\mathrm{S}) = \mu_\mathrm{cont}\sigma_0 v A_0/A_m - \alpha(T_\mathrm{R} - T_\mathrm{S}),$$

or

$$f(t) = \frac{2\mu_\mathrm{cont}\sigma_0 v}{\rho C_p} \frac{A_0}{A_m} - \frac{2\alpha}{\rho C_p}(T_\mathrm{R} - T_\mathrm{S}). \quad (23)$$

When the speed v is constant we have $x(t) = vt$ and $w(t, t') = v(t - t')/(2R)$. For this case we have shown in [9] that

$$T_q = T_{0R} + \int_0^\infty \mathrm{d}p\ f(p,t)\frac{2R}{v} \times \int_0^1 \mathrm{d}w\ \frac{qh(w)}{q + p + qp[4\pi D(2R/v)w]^{1/2}} + f(t)\frac{2R}{v}\int_0^1 \mathrm{d}w\ \frac{qq_a h(w)}{q + q_a + qq_a[4\pi D(2R/v)w]^{1/2}}. \quad (24)$$

The temperature at the rubber surface

$$T_R = T_{0R} + \int_0^\infty \mathrm{d}p\ f(p,t)\frac{2R}{v} \times \int_0^1 \mathrm{d}w\ \frac{q_1 h(w)}{q_1 + p + q_1 p[4\pi D(2R/v)w]^{1/2}} + f(t)\frac{2R}{v}\int_0^1 \mathrm{d}w\ \frac{q_a h(w)}{2 + q_a[4\pi D(2R/v)w]^{1/2}}. \quad (25)$$

If we denote

$$\Delta T_{\mathrm{visc}} = \int_0^\infty \mathrm{d}p\ f(p,t)\frac{2R}{v} \times \int_0^1 \mathrm{d}w\ \frac{q_1 h(w)}{q_1 + p + q_1 p[4\pi D(2R/v)w]^{1/2}}, \quad (26)$$

$$\Delta T_{\mathrm{cont}} = \frac{2\mu_{\mathrm{cont}}(t)\sigma_0 v}{\rho C_p}\frac{A_0}{A_m}\frac{2R}{v} \times \int_0^1 \mathrm{d}w\ \frac{q_a h(w)}{2 + q_a[4\pi D(2R/v)w]^{1/2}}, \quad (27)$$

and

$$\gamma = \frac{2\alpha}{\rho C_p}\frac{2R}{v}\int_0^1 \mathrm{d}w\ \frac{q_a h(w)}{2 + q_a[4\pi D(2R/v)w]^{1/2}}, \quad (28)$$

we get by combining (23) and (25)

$$T_R = \frac{T_{0R} + \Delta T_{\mathrm{visc}} + \Delta T_{\mathrm{cont}} + \gamma T_S}{1 + \gamma}. \quad (29)$$

The time evolution of $T_S(t)$ can be obtained approximately from (19) and (26)–(29). From (18), (19) and (29) we get

$$T_S(t) = T_{0S} + \frac{\beta}{\sqrt{\pi}}\int_0^t \mathrm{d}t'\ \frac{T_v(t') - T_S(t')}{(t - t')^{1/2}},$$

where

$$\beta = \frac{\alpha}{(1 + \gamma)(\rho' C_p' \kappa')^{1/2}},$$

and

$$T_v = T_{0R} + \Delta T_{\mathrm{visc}} + \Delta T_{\mathrm{cont}}.$$

This equation can be solved for $T_S(t)$ using Laplace transformation. We get

$$T_S(t) = T_{0S}\mathrm{erfcx}(\beta t^{1/2}) + \int_0^t \mathrm{d}t'\ \Pi(t - t')T_v(t'), \quad (30)$$

where

$$\Pi(t - t') = \frac{\mathrm{d}}{\mathrm{d}t'}\mathrm{erfcx}[\beta(t - t')^{1/2}].$$

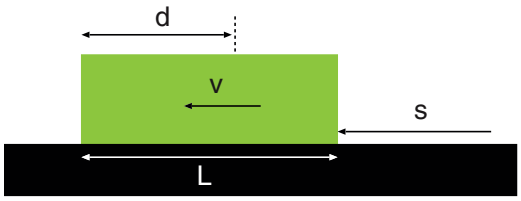

Figure 2. Rubber block (green) sliding on a substrate (road surface, black). After the sliding distance s the rubber block (and road surface) will heat up and we are interested in the temperature at the interface at different distances d from the leading edge of the block.

Here

$$\mathrm{erfcx}(x) = \mathrm{e}^{x^2}\mathrm{erfc}(x) = \frac{2}{\sqrt{\pi}}\int_x^\infty \mathrm{d}t\ \mathrm{e}^{x^2 - t^2},$$

and one can show that $\mathrm{erfcx}(x) \approx 1/(x\sqrt{\pi})$ for large x, so that $\Pi(t - t') \sim (t - t')^{-3/2}$ for large $t - t'$. We expect $T_v(t)$ to vary slowly with t for large enough t and since the factor $\Pi(t - t')$ decays for large $t - t'$ in (30) we approximate

$$T_S(t) \approx T_{0S}\mathrm{erfcx}(\beta t^{1/2}) + T_v(t)\int_0^t \mathrm{d}t'\ \Pi(t - t') = T_v + (T_{0S} - T_v)\mathrm{erfcx}(\beta t^{1/2}). \quad (31)$$

With T_R obtained from (29) and (31) we can calculate $f(t)$ using (23) and T_q from (24). Note that as $\alpha \to \infty$ then $\gamma \to \infty$ and $T_R \to T_S$ so the temperature is continuous in the macroasperity contact regions when the heat transfer coefficient α becomes very large. When $\alpha \to 0$ then $\gamma \to 0$ and $T_R \to T_{0R} + \Delta T_{\mathrm{visc}} + \Delta T_{\mathrm{cont}}$ becomes independent of the substrate temperature.

The discussion above is for an infinite sized rubber block. Consider now a finite size block with length L in the sliding direction. Let us study the heat distribution a distance d from the leading edge of the rubber block (see figure 2). Let s be the sliding distance and $t = s/v$ the sliding time. If $s < d$ the road macroasperity which occurs at a distance d from the leading edge of the rubber block at time t will have been in contact with the rubber block for the whole time period t so in this case

$$T_S(t) \approx T_v + (T_{0S} - T_v)\mathrm{erfcx}(\beta(s/v)^{1/2}) \quad \text{for } s < d. \quad (32)$$

However, if $s > d$ the macroasperity has only been in contact with the rubber block for the time d/v hence

$$T_S(t) \approx T_v + (T_{0S} - T_v)\mathrm{erfcx}(\beta(d/v)^{1/2}) \quad \text{for } s > d. \quad (33)$$

Using (29), (32) and (33) we can calculate the surface temperatures $T_R(t)$ and $T_S(t)$ in a macroasperity contact region a distance d from the leading edge of the rubber block. The calculated friction coefficient μ determines the frictional shear stress $\sigma_k = \mu p$ where p is the nominal contact pressure. Thus by varying d one can determine the rubber temperature, road macroasperity temperature and local frictional shear stress at any distance d from the rubber block leading edge.

3.2. Kinetic thermal interaction between frozen hot spots

Let us now assume that the macroasperity contact regions are circular regions with radius R and that there are N such

regions on the surface area A_0. After the sliding distance s the total surface area moved over (covered by) the macroasperity contact regions will be $Ns2R$. If $\bar{Q}$ denotes the total frictional energy per unit area after sliding distance $s = vt$ we have, if μ is constant, $\bar{Q} = \mu\sigma_0 s$. The total dissipated energy $\bar{Q}A_0$ must equal the energy dissipated in the macroasperity contact regions which equals $Q_{\rm loc}Ns2R$, where $Q_{\rm loc}$ is the energy per unit area dissipated in the macroasperity contact regions. Thus

$$\bar{Q}A_0 = Q_{\rm loc}Ns2R,$$

or

$$\bar{Q} = Q_{\rm loc}\frac{Ns2R}{A_0}.$$

Using that $A_m = N\pi R^2$ is the total macroasperity contact area, we get

$$\bar{Q} = Q_{\rm loc}\frac{A_m}{A_0}\frac{2s}{\pi R}. \tag{34}$$

If we neglect heat diffusion (resulting in what we refer to as frozen temperature spots) then when the sliding distance $s > l_{\rm av}$, where $l_{\rm av}$ is the average sliding distance before a macroasperity contact region enters into the hot track generated by another macroasperity contact region in front of it, kinetic thermal interaction will occur (see figure 1). We can take into account the kinetic interaction between hot spots in the following way: For the sliding distance $s = vt < l_{\rm av}$ there is no interaction between the hot spots and (24) and (25) correctly describe the temperature in the macroasperity contact regions. For $s > l_{\rm av}$ we include the interaction between the hot spots in an average way. That is, we smear out the flash temperature distribution laterally but we neglect the thermal diffusion so that the dependency of the background temperature on the normal coordinate z is the same (and independent of time) as that of the flash temperature. In section 3.3 we will include the (time dependent) thermal broadening (in the z-direction) of the temperature profile.

Let us write (24) as

$$T_q = T_{0\rm R} + T_{0q}(t) + \int_0^\infty {\rm d}p\ f(p,t)M(p,q) + f(t)N(q), \tag{35}$$

where $T_{0q}(t)$ is the increase in the background temperature due to the cumulative contribution from the flash temperature. When the kinetic thermal interaction is neglected as in section 3.1 $T_{0q} = 0$. However, in the present case

$$T_{0q}(t) = Q(t)\int_0^\infty {\rm d}p\ f(p,t)M(p,q) + Q(t)f(t)N(q), \tag{36}$$

where $Q(t) = 0$ for $s = vt < l_{\rm av}$ and $Q(t) = 2\bar{Q}(t)/Q_{\rm loc} = 2(A_m/A_0)(2s/\pi R)$ for $s > l_{\rm av}$. The factor 2 in this expression results from the fact that the temperature at the exit side of a macroasperity contact region is twice as high as the average flash temperature of the macroasperity contact region. Using (35) and (36) the temperature $T_{\rm R} = T_{q_a}$ at the rubber surface in the macroasperity contact regions becomes

$$T_{\rm R} = T_{0\rm R} + (1+Q)\int_0^\infty {\rm d}p\ f(p,t)M(p,q_a) + (1+Q)f(t)N(q_a). \tag{37}$$

The Q-term in this expression reflects the increase in the background temperature (which now depends on q or on the distance z into the rubber) due to frictional heating, but neglecting heat diffusion. Thus, this estimate of the background temperature will tend to overestimate the temperature increase and is accurate only at very high sliding speed v and small sliding distance s where there is no time for the temperature field to change due to thermal diffusion.

Combining (37) and (23) results again in (29) but with $\Delta T_{\rm visc}$, $\Delta T_{\rm cont}$ and γ having the additional factor $(1 + Q(t))$. Finally note that the average rubber surface temperature in the non-contact regions outside of the macroasperity contact regions is

$$\bar{T}_{\rm R} = T_{0\rm R} + T_{0q_a} = T_{0\rm R} + \frac{Q}{1+Q}(T_{\rm R} - T_{0\rm R}) = \frac{T_{0\rm R} + QT_{\rm R}}{1+Q}. \tag{38}$$

We can determine $l_{\rm av}$ as follows. Assume that the rubber block has the width W orthogonal to the sliding direction. If s is the sliding distance there will be $N = Wsc$ hot spots within the area Ws, where $c = (A_m/A_0)/(\pi R^2)$ is the concentration of hot spots. Let d denote the width of the hot track a distance s away from the macroasperity contact region from which it arises. If we neglect thermal diffusion $d = 2R$ independent of s, but when thermal diffusion is included the hot track becomes wider and $d > 2R$. As long as $W > Nd$ the tracks after the macroasperity contact regions will cover a fraction of the width of order Nd/W (see figure 1). We define $l_{\rm av}$ as the sliding distance s where $Nd/W \approx 1/2$ or scd $= 1/2$. This gives $l_{\rm av} = 1/(2cd) = (A_0/A_m)(\pi R^2/2d)$. With $d = 2R$ (i.e. neglecting the thermal broadening of the hot track) we get $l_{\rm av} = (A_0/A_m)(\pi R/4)$. At low sliding speed it is important to take into account the increase in the width of the hot tracks due to thermal diffusion. Thus, if $2(Dt)^{1/2} > R$, where the diffusion time $t = l_{\rm av}/v$, we use $d = 4(Dt)^{1/2}$. The condition $2(Dt)^{1/2} = 2(Dl_{\rm av}/v)^{1/2} = R$ with $l_{\rm av} = (A_0/A_m)(\pi R/4)$ gives $v = v* = (A_0/A_m)(\pi D/R)$. For $v < v*$ we use

$$l_{\rm av} = \frac{1}{2cd} = \frac{A_0}{A_m}\frac{\pi R^2}{8}\left(\frac{v}{Dl_{\rm av}}\right)^{1/2},$$

or

$$l_{\rm av} = \left(\frac{A_0}{A_m}\frac{\pi R^2}{8}\right)^{2/3}\left(\frac{v}{D}\right)^{1/3}.$$

To summarize:

$$l_{\rm av} = \left(\frac{A_0}{A_m}\frac{\pi R^2}{8}\right)^{2/3}\left(\frac{v}{D}\right)^{1/3}, \quad \text{for } v < \frac{A_0}{A_m}\frac{\pi D}{R} \quad \text{and}$$
$$l_{\rm av} = \frac{A_0}{A_m}\frac{\pi R}{4}, \quad \text{for } v > \frac{A_0}{A_m}\frac{\pi D}{R}.$$

3.3. Kinetic thermal interaction between hot spots

The time variation in the background temperature is due to the accumulated (or cumulative) effect of the flash temperature. In the study in section 3.2 we did not take into account that the hot track flash temperature field will broaden in the z-direction due to thermal diffusion. This broadening is characterized by the

thermal (diffusion) length $l_{\rm th} = (4Dt)^{1/2}$ and corresponding wavevector $q_{\rm th} = (2l_{\rm th})^{-1}$. In appendix A we study this effect and show that the temperature in the macroasperity contact regions can be written as:

$$T_q = T_{0\rm R} + T_{0q}(t) + \int_0^\infty {\rm d}p\ f(p,t)M(p,q) + f(t)N(q), \tag{39}$$

where

$$T_{0q}(t) \approx \int_1^\infty {\rm d}\xi\ \frac{2}{\xi^3}\left(1-{\rm e}^{-q/(q_{\rm th}\xi)}\right)T_{0,q_{\rm th}\xi}(0) + T_{0q}(0) - \int_1^\infty {\rm d}\xi\ \frac{2}{\xi^3}\frac{q}{q+q_{\rm th}\xi}T_{0,q+q_{\rm th}\xi}(0), \tag{40}$$

and

$$f(t) = \frac{2\mu_{\rm cont}\sigma_0 v}{\rho C_p}\frac{A_0}{A_m} - \frac{2\alpha}{\rho C_p}(T_{\rm R}-T_{\rm S}) = f_0 - \epsilon(T_{\rm R}-T_{\rm S}). \tag{41}$$

In (40)

$$T_{0q}(0) = Q\int_0^\infty {\rm d}p\ f(p,t)M(p,q) + Qf(t)N(q).$$

The rubber surface temperature in the macroasperity contact regions is given by (39) for $q = q_a$:

$$\begin{aligned} T_{\rm R} &= T_{0\rm R} + \int_1^\infty {\rm d}\xi\ \frac{2}{\xi^3}T_{0,q_{\rm th}\xi}(0) + \int_0^\infty {\rm d}p\ f(p,t)M(p,q_a) + f(t)N(q_a) = T_{0\rm R} \\ &+ \int_1^\infty {\rm d}\xi\ \frac{2}{\xi^3}\left[Q\int_0^\infty {\rm d}p\ f(p,t)M(p,q_{\rm th}\xi) + Qf(t)N(q_{\rm th}\xi)\right] + \int_0^\infty {\rm d}p\ f(p,t)M(p,q_a) + f(t)N(q_a) \\ &= T_{0\rm R} + \int_0^\infty {\rm d}p\ f(p,t) \times \left[Q\int_1^\infty {\rm d}\xi\ \frac{2}{\xi^3}M(p,q_{\rm th}\xi) + M(p,q_a)\right] \\ &+ f(t)\left[Q\int_1^\infty {\rm d}\xi\ \frac{2}{\xi^3}N(q_{\rm th}\xi) + N(q_a)\right]. \end{aligned} \tag{42}$$

If we write this equation as

$$T_{\rm R} = T_{0\rm R} + \Delta T_{\rm visc} + fS,$$

we get using (41)

$$T_{\rm R} = T_{0\rm R} + \Delta T_{\rm visc} + [f_0 - \epsilon(T_{\rm R}-T_{\rm S})]S,$$

or

$$T_{\rm R} = \frac{T_{0\rm R} + \Delta T_{\rm visc} + \Delta T_{\rm con} + \gamma T_{\rm S}}{1+\gamma},$$

where (see appendix A):

$$\begin{aligned} \Delta T_{\rm visc} &= \int_0^\infty {\rm d}p\ f(p,t)\frac{2R}{v} \times\left[\int_0^1 {\rm d}w\ \frac{q_1 h(w)}{q_1 + p + q_1 p[4\pi D(2R/v)w]^{1/2}} + Q\int_1^\infty {\rm d}\xi\ \frac{2}{\xi^3} \times \int_0^1 {\rm d}w\ \frac{q_{\rm th}\xi h(w)}{q_{\rm th}\xi + p + q_{\rm th}\xi p[4\pi D(2R/v)w]^{1/2}}\right], \end{aligned} \tag{43}$$

$$\begin{aligned} \Delta T_{\rm cont} &= \frac{2\mu_{\rm cont}(t)\sigma_0 v}{\rho C_p}\frac{A_0}{A_m}\frac{2R}{v} \times\left[\int_0^1 {\rm d}w\ \frac{q_a h(w)}{2 + q_a[4\pi D(2R/v)w]^{1/2}} + Q\int_1^\infty {\rm d}\xi \times \frac{2}{\xi^3}\int_0^1 {\rm d}w\ \frac{q_a q_{\rm th}\xi h(w)}{q_a + q_{\rm th}\xi + q_a q_{\rm th}\xi[4\pi D(2R/v)w]^{1/2}}\right], \end{aligned} \tag{44}$$

and

$$\gamma = \frac{2\alpha}{\rho C_p}\frac{2R}{v}\left[\int_0^1 {\rm d}w\ \frac{q_a h(w)}{2 + q_a[4\pi D(2R/v)w]^{1/2}} + Q\int_1^\infty {\rm d}\xi \times \frac{2}{\xi^3}\int_0^1 {\rm d}w\ \frac{q_a q_{\rm th}\xi h(w)}{q_a + q_{\rm th}\xi + q_a q_{\rm th}\xi[4\pi D(2R/v)w]^{1/2}}\right]. \tag{45}$$

3.4. Relation between T_q and $T(z)$

The theory above predicts the temperature $T_q(t)$ but we are really interested in $T(z,t)$ which can be obtained from $T_q(t)$ as follows. We have (we suppress the time-dependency):

$$T_q = \frac{\int_0^\infty {\rm d}z\ T(z){\rm e}^{-2qz}}{\int_0^\infty {\rm d}z\ {\rm e}^{-2qz}} = 2q\int_0^\infty {\rm d}z\ T(z){\rm e}^{-2qz}.$$

We can obtain $T(z)$ from this equation by 'inverting' the equation numerically. Here we instead present an approximate procedure to obtain $T(z)$ from T_q. We note that

$$T_q = 2q\int_0^\infty {\rm d}z\ T(z){\rm e}^{-2qz} \approx 2q\int_0^{1/2q} {\rm d}z\ T(z).$$

Thus

$$\frac{\partial}{\partial q}\left(\frac{T_q}{2q}\right) \approx -\frac{1}{2q^2}T(z=1/2q),$$

or

$$-q^2\frac{\partial}{\partial q}\left(\frac{T_q}{q}\right) \approx T(z=1/2q),$$

or

$$T(z=1/2q) \approx T_q - q\frac{\partial T_q}{\partial q}, \tag{46}$$

from which $T(z)$ can be obtained by numerical derivation of T_q. If we write

$$q = q_0{\rm e}^{\mu},$$

and denote T_q with T_μ for simplicity, we get

$$T(z=1/2q) \approx T_\mu - \frac{\partial T_\mu}{\partial \mu}. \tag{47}$$

3.5. Energy conservation

During sliding most of (and in the theory all) the frictional energy is transferred into heat. If the friction coefficient is approximately constant during the sliding distance s, the total frictional energy per unit surface area is $\mu_k p v t$, where $t = s/v$ is the sliding time. The transfer of heat energy to the substrate

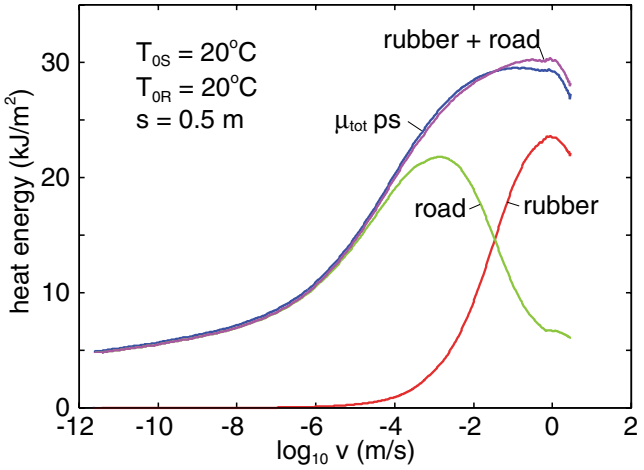

Figure 3. Red line: the heat energy (per unit nominal surface contact area A_0) stored in the rubber at the end of the sliding process. Green line: the heat energy transferred to the road divided by A_0. Pink line: sum of the above mentioned contributions. Blue line: the dissipated rubber friction energy (divided by A_0), $\mu_{\rm tot}ps$, where $s = 0.5$ m is the sliding distance. The rubber initial temperature $T_{0R} = 20\,^\circ$C and the road initial temperature $T_{0R} = 20\,^\circ$C. The blue and pink lines almost overlap, i.e. energy conservation is almost obeyed which is a non-trivial result because of the approximate treatment of the heat diffusion.

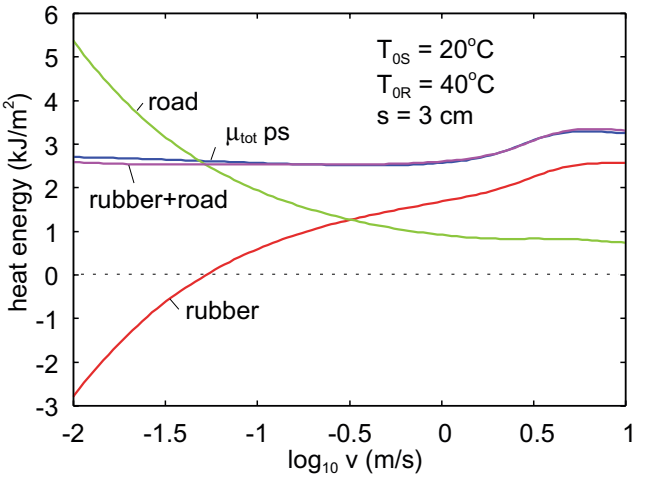

Figure 4. Same as in figure 3 but for $T_{0R} = 40\,^\circ$C and for the sliding distance $s = 3$ cm. Note that the blue and pink lines almost overlap, i.e. energy conservation is almost obeyed which is a non-trivial result because of the approximate treatment of the heat diffusion.

(road) equals $\alpha(T_{\rm R} - T_{\rm S})A_m t$ and the heat energy stored per unit surface area in the rubber equals

$$\rho C_p \int_0^\infty {\rm d}z\, [T(z,t) - T_{0R}] = \rho C_p \lim_{q\to 0} \frac{T_q(t)}{2q}.$$

Thus

$$\mu_k ps = \alpha(T_{\rm R} - T_{\rm S})\frac{A_m s}{v} + \rho C_p \lim_{q\to 0}\frac{T_q(t)}{2q}. \qquad (48)$$

This energy conservation law is very well satisfied in our numerical calculations. This is illustrated in figure 3 which shows the various contributions to the dissipated energy when a rubber block has been sliding $s = 0.5$ m on an asphalt road surface (using the same system parameters as in section 4). The rubber and road initial temperatures are both 20 °C. The green line is the heat energy transferred to the road divided by A_0 (first term on the right hand side in (48)). The red line shows the heat energy (per unit nominal surface contact area A_0) stored in the rubber at the end of the sliding process (second term on the right hand side in (48)) and the pink line is the sum of both. The blue line is the dissipated rubber friction energy (divided by A_0), $\mu_{\rm tot}ps$. The blue and pink lines almost overlap, i.e. energy conservation is almost obeyed which is a non-trivial result because of the approximate treatment of the heat diffusion. Note that at low sliding speed, $v < 10^{-4}$ m s^{-1}, nearly all the frictional energy is transferred to the road which implies that negligible frictional heating of the rubber block occurs, while for $v \approx 2$ cm s^{-1} about half of the frictional energy is transferred to the road. As the sliding distance increases a larger and larger fraction of the frictional energy will be transferred to the road.

Figure 4 shows similar results as in figure 3, but now for $T_{0R} = 40\,^\circ$C and $T_{0S} = 20\,^\circ$C (unchanged). The sliding distance $s = 3$ cm as typical for ABS (anti-lock braking system) braking. In this case, for low sliding speed there is a large transfer of heat energy from the rubber to the road. This results from the long contact time $t = s/v$ and from the fact that the rubber block is hotter than the substrate, resulting in a flow of heat energy to the road. Nevertheless, the sum of the heat energy transferred to the road and the heat energy in the rubber is again very close to the frictional energy dissipation, i.e. energy conservation is satisfied to a good approximation.

4. Numerical results

We now present numerical results to illustrate the theory. All results are for a rubber tread compound (denoted A) sliding on an asphalt road surface. The surface roughness power spectrum of the road surface and the viscoelastic modulus of the rubber compound are given below in section 5. In all the calculations we assume the nominal contact pressure $\sigma_0 = 0.065$ MPa, which is similar to what is used in some of our friction experiments. The rubber block is $L = 5$ cm long in the sliding direction. The rubber heat conductivity $\kappa = 0.23$ W mK^{-1}, heat capacity $C = 1650$ J kg^{-1} K^{-1} and mass density $\rho = 1200$ kg m^{-3}. The road heat conductivity $\kappa = 1.0$ W mK^{-1}, heat capacity $C = 700$ J kg^{-1} K^{-1} and mass density $\rho = 2700$ kg m^{-3}. The road-rubber heat transfer coefficient $\alpha = 10^7$ W m^{-2} K^{-1} is assumed velocity independent and so large that the temperature is (almost) continuous in the macroasperity contact regions. The assumption that the surface temperature is the same on the rubber and road side of the contact is often made, but we note that our theory also allows for a discontinuity in the temperature, which would be the case if the heat transfer coefficient is much smaller than assumed above (see [9]).

In the numerical results presented below we assume that there is a contribution to the friction coefficient from the area of contact, $\mu_{\rm cont}(v,T) = (\tau_f(v,T)/\sigma_0)(A_1/A_0)$. The area of contact A_1 and the frictional shear stress $\tau_f(v,T)$

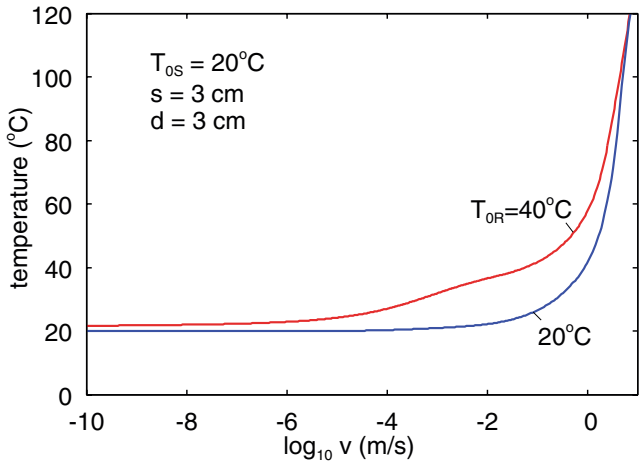

Figure 5. The temperature in the macroasperity contact regions a distance $d = 3$ cm from the leading edge of the rubber block after sliding the distance $s = 3$ cm as a function of the sliding speed. The rubber initial temperature is $T_{0R} = 20\,^{\circ}$C (blue curve) and 40 °C (red curve), while the road (or substrate) initial temperature is $T_{0S} = 20\,^{\circ}$C.

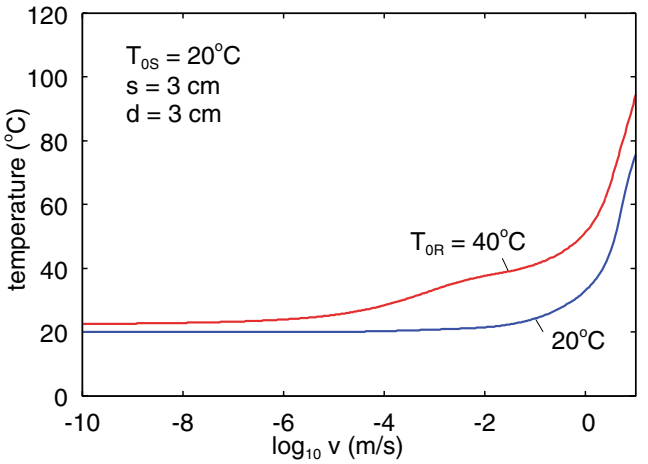

Figure 6. The average rubber surface temperature a distance $d = 3$ cm from the leading edge of the rubber block after sliding the distance $s = 3$ cm as a function of the sliding speed. The rubber initial temperature is $T_{0R} = 20\,^{\circ}$C (blue curve) and 40 °C (red curve), while the road (or substrate) initial temperature is $T_{0S} = 20\,^{\circ}$C.

depends on sliding velocity v and on temperature T. Here we use the $\tau_f(v, T)$ determined in [23, 24] by comparing theory to experiment. As a function of the logarithm of the sliding velocity, $\tau_f(v, T)$ was found to be a wide Gaussian-like curve with a full width at half maximum of about 5 velocity decades. The physical origin of the frictional shear stress may be bonding-stretching-debonding cycles of rubber molecules at the sliding interface, as first suggested by Schallamach [25] and considered in more detail in [26, 27]. The initial ($t = 0$) road temperature is always $T_{0S} = 20\,^{\circ}$C and the initial rubber block temperature T_{0R} is either 20 °C or 40 °C.

During ABS breaking of a car the tread blocks in the tire-road footprint slide at most few cm and in this section we present results for the sliding distance $s = 3$ cm. (In tire applications the nominal contact pressure is typically ∼0.3 MPa, i.e. much larger than we use here. However, in the experiments presented in the next section the nominal contact pressure is ≈0.065 MPa and we use the same value here to be able to compare with the results in section 5.)

Figure 5 shows the temperature in the macroasperity contact regions a distance $d = 3$ cm from the leading edge of the rubber block, as a function of the sliding speed. The initial rubber temperature is $T_{0R} = 20\,^{\circ}$C (blue curve) or 40 °C (red curve) and the initial road (or substrate) temperature is $T_{0S} = 20\,^{\circ}$C. When the road and rubber initial temperatures both equal 20 °C, the temperature in the macroasperity contact regions stays close to 20 °C until the sliding velocity reaches ≈10 cm s^{-1}, after which the temperature rapidly increases reaching about 100 °C at ≈3 m s^{-1}.

When the rubber initial temperature is 40 °C, the temperature for sliding speeds $v < 1\,\mu$m s^{-1} is again close to the road initial temperature. The reason for this is the ∼5 times higher thermal conductivity of the road as compared to the rubber. (In addition, the leading edge of the rubber block continuously moves into contact with the 'cold' road surface in front of the rubber block, which (for long sliding distance) is another reason for why the temperature at the rubber surface

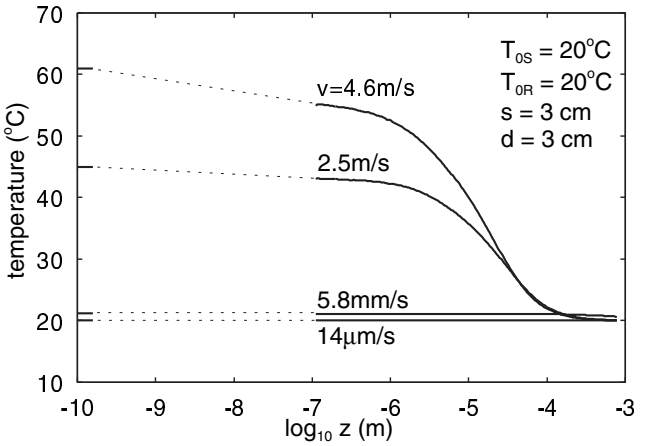

Figure 7. The temperature (at $d = 3$ cm) as a function of the distance z from the surface in a macroasperity contact region for different sliding speeds, after sliding the distance $s = 3$ cm. Note that the temperature is maximal at the surface for the two higher sliding speeds ($v = 4.6$ m s^{-1} and 2.5 m s^{-1}) while staying nearly constant for the two lower sliding speeds. The rubber and road initial temperatures are $T_{0R} = 20\,^{\circ}$C and $T_{0S} = 20\,^{\circ}$C.

may be closer to the road surface.) However, for sliding speeds $v > 100\,\mu$m s^{-1} the temperature in the macroasperity contact region approaches the initial rubber temperature, 40 °C and then for $v > 10$ cm s^{-1}, the temperature rapidly increases as for the case where the initial road and rubber temperatures are both 20 °C.

Figure 6 shows similar results as in figure 5 but now for the average rubber surface temperature, a distance $d = 3$ cm from the leading edge of the rubber block (the rubber surface temperature is averaged in the y-direction, orthogonal to the sliding direction).

Figure 7 shows the temperature (at $d = 3$ cm) as a function of the distance from the surface in a macroasperity contact region for different sliding speeds. The initial rubber and road temperatures are both 20 °C. Note that the temperature is maximal at the surface for the two higher sliding speeds

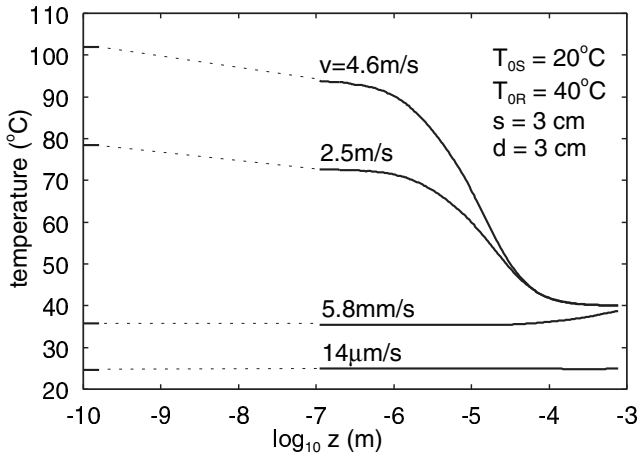

Figure 8. The temperature (at $d = 3$ cm) as a function of the distance z from the surface in a macroasperity contact region for different sliding speeds. Note that the temperature is maximal at the surface for the two higher sliding speeds ($v = 4.6\,\mathrm{m\,s^{-1}}$ and $2.5\,\mathrm{m\,s^{-1}}$) while staying nearly constant for the two lower sliding speeds. The rubber and road initial temperatures are $T_{0R} = 40\,^{\circ}\mathrm{C}$ and $T_{0S} = 20\,^{\circ}\mathrm{C}$.

($v = 4.6\,\mathrm{m\,s^{-1}}$ and $2.5\,\mathrm{m\,s^{-1}}$) and nearly constant and equal to $\approx 20\,^{\circ}\mathrm{C}$ for the two lower sliding speeds.

Figure 8 shows similar results as in figure 7 but now when the rubber initial temperature equal $T_{0R} = 40\,^{\circ}\mathrm{C}$. Note again that the temperature is maximal at the surface for the two higher sliding speeds ($v = 4.6\,\mathrm{m\,s^{-1}}$ and $2.5\,\mathrm{m\,s^{-1}}$) and nearly constant for the two lower sliding speeds. However, in this case the temperature for the three highest velocities approaches $40\,^{\circ}\mathrm{C}$ at $z \approx 1$ mm. This effect is due to the short rubber-road sliding (or contact) time $t = s/v$ at the higher velocities and due to the finite time $t \approx l^2/D$ necessary for heat diffusion to transfer energy over some distance l.

5. Comparison of theory with experiment

At the Bridgestone lab we have developed a rubber friction tester where a rubber block is slid on a circular asphalt road track. Using this new set-up we have studied the temperature distribution on the road surface behind the rubber block. The temperature measurements were performed using an infrared camera. Figure 9 shows the rubber block used in the study of the temperature development and figure 10 shows the temperature distribution after a sliding distance of order a few meter. We note that the temperature is measured by the infrared camera with an inclination angle of $\approx 70^{\circ}$ relative to the road surface normal (and $\approx 120^{\circ}$ from the sliding direction in the horizontal plane) and for this reason only the road temperature close to the top regions of the highest asperities is observed. Thus, the average road surface temperature will be lower than the temperatures measured with the present set-up. We note that the macroasperity contact area in the present case is of order 10% of the nominal contact area, so if the road temperature at the trailing edge of the rubber road contact would be measured along the surface normal direction, the average temperature would (at high sliding speed where the heat diffusion broadening of the hot temperature spots is

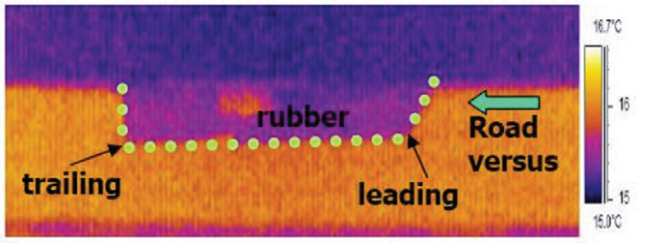

Figure 9. The rubber block used in the experimental study of sliding friction and temperature development, during sliding on an asphalt road surface.

small) be of order $\approx 0.9T_{0S} + 0.1T_S$. However, at the near grazing incidence we use the measured average road surface temperature will be closer to the temperature T_S prevailing in the macroasperity contact regions at the trailing edge.

The power spectrum of the asphalt road track used in this study is shown in figure 11. The blue line is the measured data (from engineering line-scan instrument) and the red line the extrapolated power spectrum. The low and large cut-off wavevectors, q_0 and q_1, used in the theory are indicated.

Figure 12 shows the real and imaginary part of the viscoelastic modulus of the rubber tread compound A used in the experimental study and in the theory calculations. The shown modulus was obtained at very small strain amplitude (0.04% strain) where linear response is stricly obeyed. We also performed strain sweeps to large strain (of order 100% strain) at several different temperatures. In the theory calculations we take into account the strain softening which occurs at the typical strain prevailing in the rubber-road asperity contact regions.

In this section we present experimental data and compare the results with the theory developed above. We also present theoretical results for the temperature field in the rubber which cannot be probed experimentally with the present set-up. Figure 13 shows the measured maximum temperatures on the road surface (in the 'area of interest' in figure 10) for two compounds A and C as a function of the sliding speed when the normal load is $F_N = 64\,\mathrm{N}$ and $F_N = 128\,\mathrm{N}$. The length of the rubber block is about $L_x = 4.5$ cm and the width $L_y = 2.5$ cm. The load $F_N = 64\,\mathrm{N}$ corresponding to about $\sigma_0 \approx 0.06$ MPa nominal contact pressure. Figure 14 shows the measured friction coefficient for the same systems as figure 13.

We now present calculated results for the rubber compound A for the same road surface as used in the experiment above. We first show the temperature distribution in the rubber block after sliding a distance s between 0.03 m and 1 m. After sliding a distance s the rubber block (and road surface) will heat up and we are interested in the temperature at the interface at different distances d from the leading edge of the block (see figure 2).

Figure 15 shows the rubber macroasperity (surface) temperature T_R (nearly equal to the road asperity contact temperature T_S) as a function of sliding speed. Results are shown at the trailing edge of the rubber block ($d = 5$ cm) for the sliding distances $s = 0.03$, 0.1, 0.25, 0.5 and 1 m. Note that the temperature change is rather small when the sliding distance increases from 0.5 and 1 m. The reason for this is that

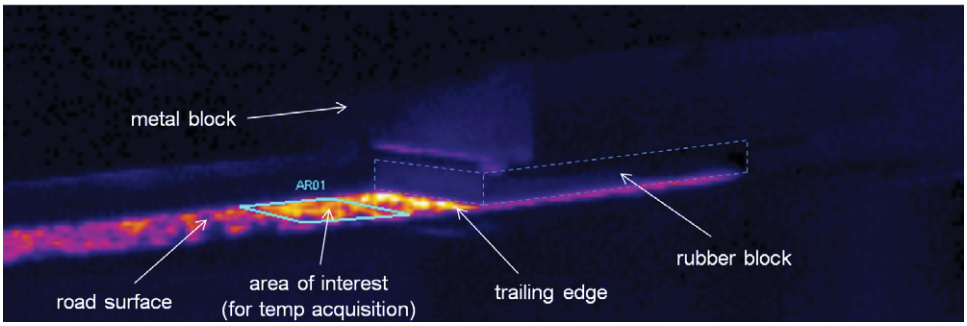

Figure 10. Snapshot picture (infrared camera) of the temperature distribution resulting when the rubber block (see figure 9) is slid a few meter on an asphalt road surface. The maximum and the average temperature on the road surface quoted below refer to the 'area of interest', a rectangular area (2 cm × 1.5 cm) located a few cm behind the trailing edge of the rubber-road contact area. We did not study in detail the temperature right at the edge of contact since rubber debris, not yet fully detached from the rubber block, resulted in a local temperature at the trailing edge which fluctuated rapidly in space and time.

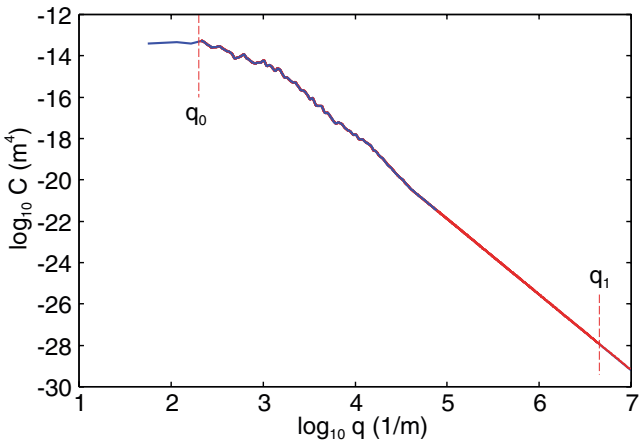

Figure 11. The surface roughness power spectrum of an asphalt road surface. The blue line is the measured data (from engineering line-scan instrument) and the red line extrapolated power spectrum. The small and large cut-off wavevectors, q_0 and q_1, used in the analysis are indicated.

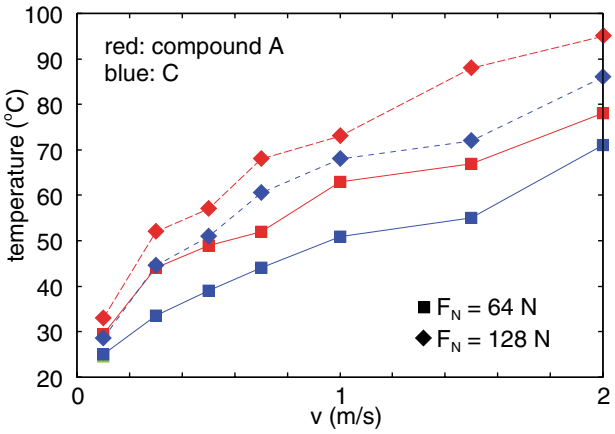

Figure 13. The measured maximum temperature on the road surface at the trailing edge of the sliding rubber block, as a function of the sliding speed for two different tread compounds A and C and for the normal load $F_N = 64$ N and 128 N. The sliding distance $s \approx 3$ m.

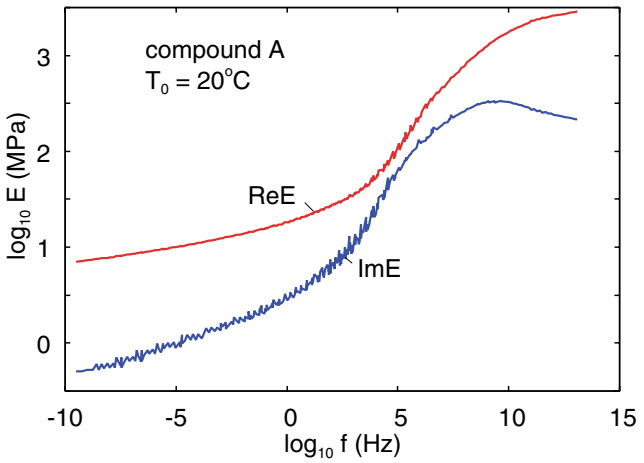

Figure 12. The real and imaginary part of the viscoelastic modulus of a rubber tread compound A. The reference temperature $T_0 = 20\,^{\circ}$C. The shown modulus was obtained with such a small strain amplitude (0.04% strain) that linear response is stricly obeyed.

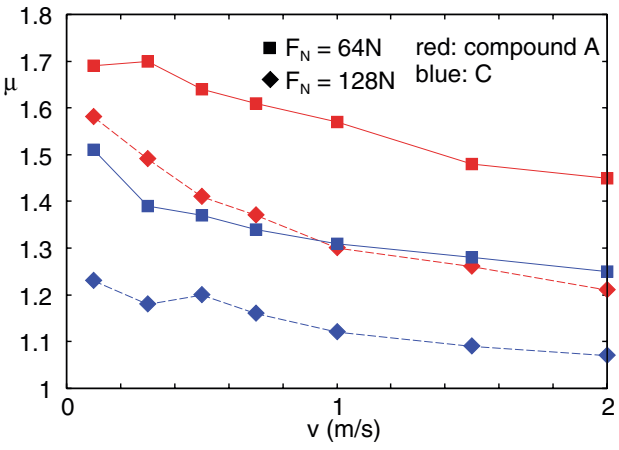

Figure 14. The measured friction coefficient as a function of the sliding speed for two different tread compounds A and C and for the normal load $F_N = 64$ N and 128 N. The sliding distance $s \approx 3$ m.

as the rubber block heats up, the heat transfer to the road surface increases (because the road surface is always at the initial temperature 20 °C at the leading edge of the block-road contact region) and after a sliding distance of order 1 m the frictional

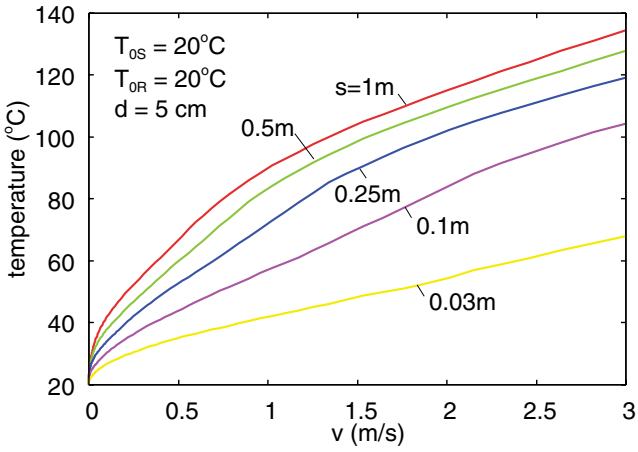

Figure 15. The macroasperity contact region temperature as a function of sliding speed. Results are shown for sliding distances $s = 0.03$, 0.1, 0.25, 0.5 and 1 m at the trailing edge of the rubber block ($d = 5$ cm). For the nominal contact pressure $p = 0.065$ MPa and road and rubber initial temperature $T_{0S} = T_{0R} = 20\,^{\circ}$C.

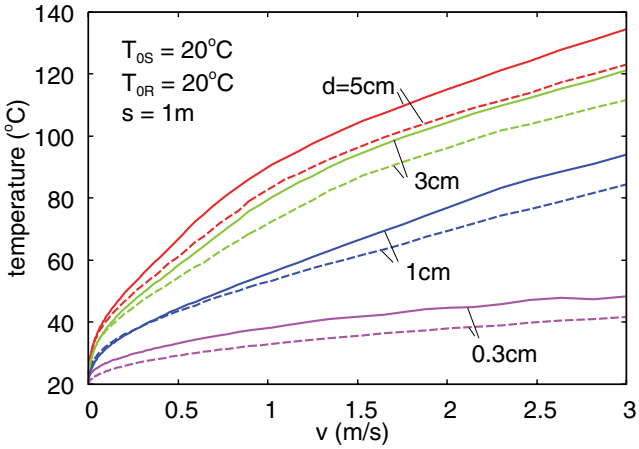

Figure 16. The rubber temperature in the macroasperity contact regions (solid lines) and the average rubber surface temperature (dashed lines) at different distances d from the leading edge of the rubber block, after the sliding distance $s = 1$ m. For the nominal contact pressure $p = 0.065$ MPa and road and rubber initial temperature $T_{0S} = T_{0R} = 20\,^{\circ}$C.

energy dissipated per unit time nearly equals the transfer of heat energy per unit time to the road. Figure 15 shows that the temperature in the macroasperity contact regions, after sliding 1 m at the speed $v = 2\,\mathrm{m\,s^{-1}}$, is about 110 °C at the trailing edge. This is higher than what we measure on the road surface which gives ≈80 °C. The higher temperature predicted by the theory is expected partly because in the experiment the temperature is measured a few cm away from the trailing edge and partly because the macroasperity contact regions are very small (of order 1 mm in diameter) and the resolution of the infrared camera may not be high enough to resolve the temperature on the length scale of 1 mm.

Figure 16 shows the rubber temperature in the macroasperity contact regions (solid lines) and the average rubber surface temperature (dashed lines) at different distances d from the leading edge of the rubber block, after the sliding distance $s = 1$ m. Note that the temperature at the trailing edge of the rubber-road nominal contact region is much higher than at the leading edge of the contact region. Again, this is due to the heating of the road surface during the time it is in contact with the rubber block.

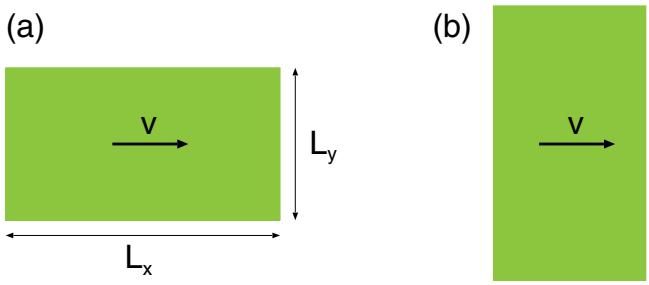

Figure 17. Frictional heating is more important when the rubber block slides parallel the long side L_x as in (a), as compared to along the short side L_y as in (b).

One important conclusion from figure 16 is that rubber friction at high enough sliding speeds, where thermal effects are important, will depend on the orientation of a rectangular rubber block with the sides L_x and L_y. Thus, if $L_x > L_y$ the road asperities will stay in contact with the rubber block for a longer time and heat up more than if the block slides in the y-direction. We conclude that frictional heating is more important when the block slides parallel to the long side of the block (see figure 17 where $L_x \approx 4.5$ cm and $L_y \approx 2.5$ cm). We have indeed observed this effect as can be seen in figure 18, which shows results for three different rubber compounds, A′, B′ and C′. Thus, frictional heating results in a kinetic friction force which depends on the orientation of the sliding block, thus violating the first friction 'law' of Leonardo da Vinci [28]. The second law of Leonardo da Vinci, namely that the friction force is independent of the normal load (or nominal contact pressure), is of course also violated when frictional heating becomes important at higher sliding velocities.

The spatial variation of the temperature on the bottom surface of the rubber block will result in local rubber wear rates which depend on the distance d from the leading edge of the contact. The non-uniform temperature profile will influence the shape of the rubber surface profile after run-in.

Finally, let us present some calculated results for the temperature field which cannot be measured using our present experimental set-up. Figure 19 shows the rubber macroasperity temperature (red lines) and the average rubber surface temperature (blue lines) as a function of sliding speed, after sliding the distance $s = 1$ m. Results are shown for $d = 5$ cm and $d = 0.1$ cm.

Figure 20 shows the temperature (at $d = 1$ cm) as a function of the distance from the surface in a macroasperity contact region for different sliding speeds. Note that at the lowest sliding speed the temperature is nearly constant and close to the initial rubber and road temperature (20 °C). At the highest sliding speed the sliding time s/v is rather short and the heat diffusion length $l \approx (Ds/v)^{1/2}$ so short that the temperature at $z \approx 1$ mm is nearly the same as the initial rubber (and road) temperature (20 °C). However, for $v = 43\,\mathrm{mm\,s^{-1}}$ the temperature profile extends deeper into the rubber block and $T \approx 25\,^{\circ}$C at $z \approx 1$ mm.

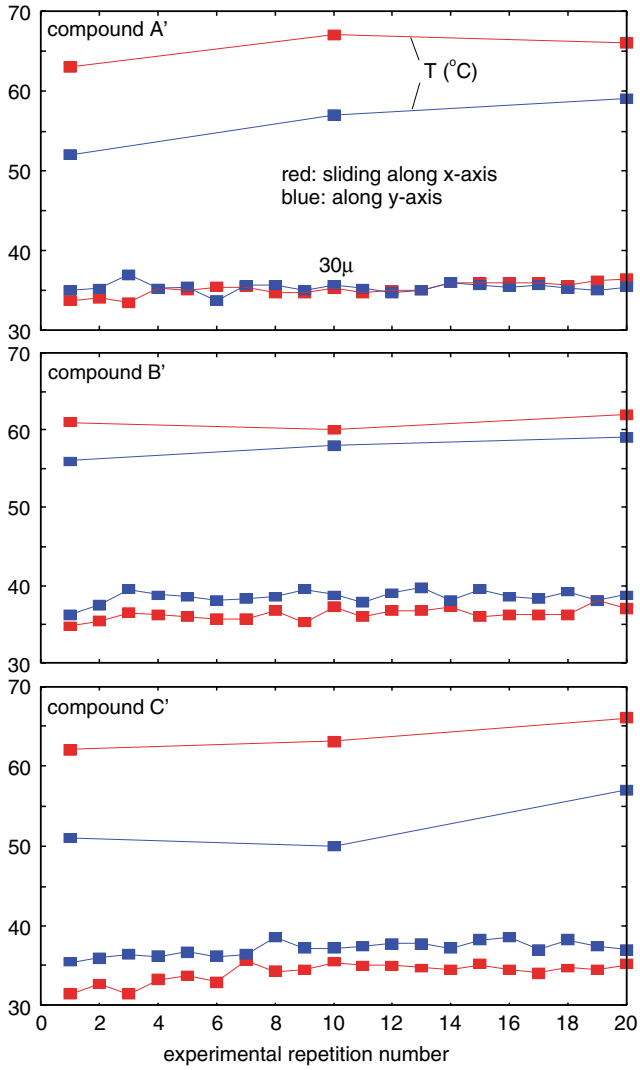

Figure 18. The average temperature on the road surface within the 'area of interest' at the trailing edge of the rubber-road contact area (see figure 10) as a function of the number of repetitions. The red line is for sliding along the x-axis and the blue line along the y-axis (see figure 17). Also shown are the friction coefficients (times a factor of 30). For compound A′, B′ and C′.

6. Summary

We have derived equations which describe the frictional heating for arbitrary (non-uniform) motion and taking into account that some of the frictional energy is produced inside the rubber due to the internal friction in rubber. The heat energy transfer at the sliding interface is described by a heat transfer coefficient α which can be measured experimentally and calculated theoretically. The theory is valid for solids with arbitrary thermal properties and sliding conditions. We have presented numerical results for the space and time variation of the temperature distribution during sliding of a rubber block on a road surface. In a typical case, after sliding a distance of order $\sim$1 m s^{-1} the temperature at the road-rubber interface changes very slowly, i.e. a quasi-stationary state prevails.

We have developed a new friction tester and performed experiments where a rubber block is slid on an asphalt road track. Using an infrared camera we have measured the temperature distribution on the road surface at the trailing edge of the rubber-road contact. The measured temperature increase is consistent with the theory predictions.

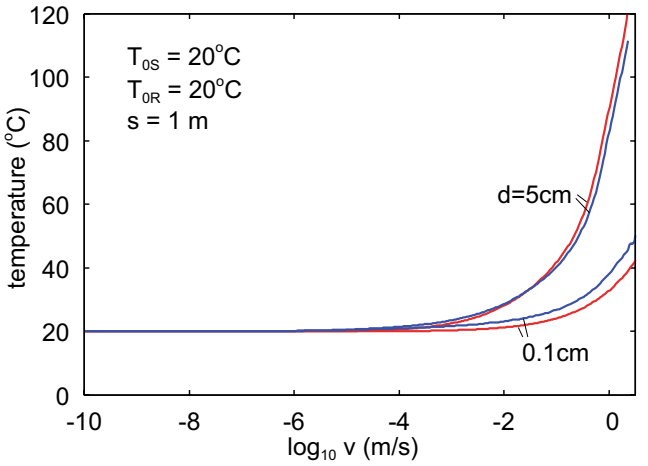

Figure 19. The rubber macroasperity (surface) temperature (red lines) and the average rubber surface temperature (blue lines) as a function of sliding speed, after sliding the distance $s = 1$ m. Results are shown for $d = 5$ cm and $d = 0.1$ cm. For the nominal contact pressure $p = 0.065$ MPa and road and rubber initial temperature $T_{0R} = T_{0S} = 20\,^{\circ}$C.

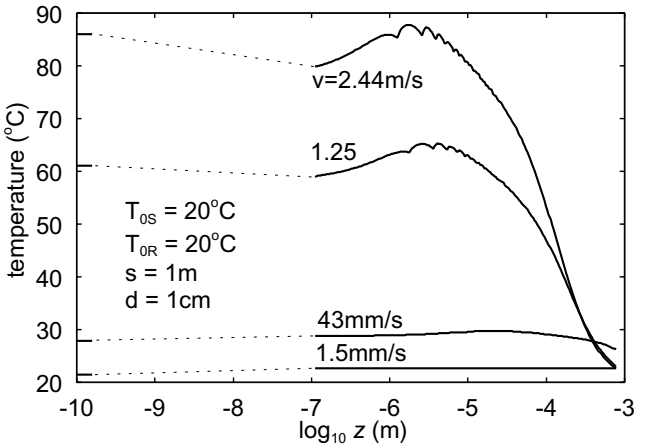

Figure 20. The temperature (at $d = 1$ cm) as a function of the distance from the surface in a macroasperity contact region at different sliding speeds. For the nominal contact pressure $p = 0.065$ MPa and road and rubber initial temperatures $T_{0R} = T_{0S} = 20\,^{\circ}$C.

Acknowledgments

The research work was performed within a Reinhart-Koselleck project funded by the Deutsche Forschungsgemeinschaft (DFG). The authors would like to thank DFG for the project support under the reference German Research Foundation DFG-Grant: MU 1225/36-1. This work is supported in part by COST Action MP1303.

Appendix A. Kinetic thermal interaction between hot spots

The time variation in the background temperature is due to the accumulated (or cumulative) effect of the flash temperature.

In the study in section 3.2 we did not take into account that the (laterally smeared out) hot track flash temperature field will broaden in the z-direction due to thermal diffusion. To study this effect let us divide the sliding distance $s = vt$ into N equal segments: $s = N\Delta s = Nv\Delta t$. We can then write (36) as

$$T_{0q}(t) = \sum_{n=1}^{N} \Delta T_{0q}(t_n),$$

where

$$\Delta T_{0q}(t_n) = \Delta Q \int_0^\infty \mathrm{d}p\ f(p, t_n) M(p, q) + \Delta Q f(t_n) N(q), \tag{A1}$$

where $\Delta Q = 2(A_m/A_0)(2\Delta s/\pi R) = Q/N$. In the equation above $\Delta T_{0q}(t_n)$ is the contribution to the temperature at time t from the flash temperature created during the sliding interval $\Delta s = v\Delta t$. In the study above this temperature contribution was assumed to have the same z-variation as the flash temperature, i.e. the thermal diffusion was neglected. However, in reality during the time from $t_n = n\Delta t$ to $t = N\Delta t$ the temperature profile will broaden. Thus we need to replace $\Delta T_{0q}(t_n)$ with $\Delta T_{0q}(t, t_n)$. We will neglect the variation of the friction coefficient with time which implies that $\Delta T_{0q}(t, t_n)$ only depends on $t - t_n$ so we can write it as $\Delta T_{0q}(t - t_n)$.

In the limit $N \to \infty$ we can consider n as a continuous variable and write

$$T_{0q}(t) = \int_0^N \mathrm{d}n\ \Delta T_{0q}(t - t_n).$$

Writing $t_n = n\Delta t = t'$ we get

$$T_{0q}(t) = \frac{1}{\Delta t}\int_0^t \mathrm{d}t'\ \Delta T_{0q}(t - t') = \frac{1}{t}\int_0^t \mathrm{d}t'\ N\Delta T_{0q}(t - t') = \frac{1}{t}\int_0^t \mathrm{d}t'\ N\Delta T_{0q}(t') = \frac{1}{t}\int_0^t \mathrm{d}t'\ T_{\mathrm{N}q}(t'), \tag{A2}$$

where $T_{\mathrm{N}q} = N\Delta T_{0q}$. Note that $T_{0q}(0) = T_{\mathrm{N}q}(0)$.

We will now show how the thermal broadening of the background temperature profile can be included in an approximate way. Let $T_0(z, t)$ be defined so that

$$T_{\mathrm{N}q}(t) = \frac{\int_0^\infty \mathrm{d}z\ T_0(z, t)\mathrm{e}^{-2qz}}{\int_0^\infty \mathrm{d}z\ \mathrm{e}^{-2qz}}. \tag{A3}$$

Thus $T_0(z, t)$ is the temperature distribution at time t arising from the flash temperature generated in the time interval Δt at $t = 0$, times the factor $N = t/\Delta t$.

In the contact area outside of the macroasperity contact regions the temperature $T_0(z, t)$ evolves with time as:

$$T_0(z, t) = \frac{1}{(4\pi Dt)^{1/2}}\int_0^\infty \mathrm{d}z'\ T_0(z', 0) \times \left[\exp\left(-\frac{(z - z')^2}{4Dt}\right) + \exp\left(-\frac{(z + z')^2}{4Dt}\right)\right].$$

Note that from this equation we get

$$\int_0^\infty \mathrm{d}z\ T_0(z, t) = \int_0^\infty \mathrm{d}z\ T_0(z, 0),$$

so the thermal energy is conserved as must be the case.

We can obtain an approximate expression for $T_{0q}(t)$ as follows. For $z < l_{\mathrm{th}}$, where the thermal (diffusion) length $l_{\mathrm{th}} = (4Dt)^{1/2}$, we have

$$T_0(z, t) \approx \frac{1}{(4\pi Dt)^{1/2}}\int_0^{l_{\mathrm{th}}} \mathrm{d}z'\ T_0(z', 0)(1 + 1) \approx \frac{2}{(4\pi Dt)^{1/2}}\int_0^\infty \mathrm{d}z'\ T_0(z', 0)\mathrm{e}^{-z'/l_{\mathrm{th}}}, \tag{A4}$$

while for $z > l_{\mathrm{th}}$

$$T_0(z, t) \approx T_0(z, 0). \tag{A5}$$

If we introduce

$$q_{\mathrm{th}} = (2l_{\mathrm{th}})^{-1},$$

we can also write (A4) as

$$T_0(z, t) \approx \frac{2}{(4\pi Dt)^{1/2}}\int_0^\infty \mathrm{d}z'\ T_0(z', 0)\mathrm{e}^{-2q_{\mathrm{th}}z'} = \frac{2}{(4\pi Dt)^{1/2}}\frac{1}{2q_{\mathrm{th}}}T_{0q_{\mathrm{th}}}(0) = \frac{2}{\sqrt{\pi}}T_{0q_{\mathrm{th}}}(0). \tag{A6}$$

Note in particular that the temperature at the surface $z = 0$ is

$$T_0(0, t) = \frac{2}{\sqrt{\pi}}T_{0q_{\mathrm{th}}}(0),$$

which depends on time only via $q_{\mathrm{th}} = (2l_{\mathrm{th}})^{-1} = (Dt)^{-1/2}/4$.

Let us now calculate $T_{\mathrm{N}q}(t)$. Using (A3), (A5) and (A6) gives

$$\begin{aligned} T_{\mathrm{N}q}(t) &= 2q\int_0^\infty \mathrm{d}z\ T_0(z, t)\mathrm{e}^{-2qz} \\ &\approx 2q\int_0^{l_{\mathrm{th}}} \mathrm{d}z\mathrm{e}^{-2qz}\frac{2}{\sqrt{\pi}}T_{0q_{\mathrm{th}}}(0) + 2q\int_{l_{\mathrm{th}}}^\infty \mathrm{d}z\ T_0(z, 0)\mathrm{e}^{-2qz} \\ &= \left(1 - \mathrm{e}^{-q/q_{\mathrm{th}}}\right)\frac{2}{\sqrt{\pi}}T_{0q_{\mathrm{th}}}(0) + 2q\int_0^\infty \mathrm{d}z\ T_0(z, 0)\mathrm{e}^{-2qz} \\ &\quad -2q\int_0^{l_{\mathrm{th}}} \mathrm{d}z\ T_0(z, 0)\mathrm{e}^{-2qz}. \end{aligned} \tag{A7}$$

The last integral in (A7) can be calculated approximately as follows:

$$2q\int_0^{l_{\mathrm{th}}} \mathrm{d}z\ T_0(z, 0)\mathrm{e}^{-2qz} \approx \frac{2q}{2(q + q_{\mathrm{th}})}2(q + q_{\mathrm{th}}) \times \int_0^\infty \mathrm{d}z\ T_0(z, 0)\mathrm{e}^{-2q_{\mathrm{th}}z}\mathrm{e}^{-2qz} = \frac{q}{q + q_{\mathrm{th}}}T_{0,q+q_{\mathrm{th}}}(0).$$

Thus we get

$$T_{\mathrm{N}q}(t) \approx \left(1 - \mathrm{e}^{-q/q_{\mathrm{th}}}\right)\frac{2}{\sqrt{\pi}}T_{0q_{\mathrm{th}}}(0) + T_{0q}(0) - \frac{q}{q + q_{\mathrm{th}}}T_{0,q+q_{\mathrm{th}}}(0). \tag{A8}$$

Note that as $t \to 0$ the left hand side in (A8) approaches $T_{0q}(0)$ while the right hand side approaches $(2/\sqrt{\pi})T_{0q}(0)$. Hence we must replace $2/\sqrt{\pi}$ with unity in order to get this limiting case correct. The same result follows from energy conservation (see below). Thus we get

$$T_{\mathrm{N}q}(t) \approx \left(1 - \mathrm{e}^{-q/q_{\mathrm{th}}}\right)T_{0q_{\mathrm{th}}}(0) + T_{0q}(0) - \frac{q}{q + q_{\mathrm{th}}}T_{0,q+q_{\mathrm{th}}}(0). \tag{A9}$$

Note that as $t \to 0$ then $q_{\rm th} \to \infty$ and (A9) gives $T_{{\rm N}q}(0) = T_{0q}(0)$ so (A9) in this limit is exact. Similarly, as $t \to \infty$ then $q_{\rm th} \to 0$ and (A9) gives $T_{{\rm N}q}(t) \to T_{0q_{\rm th}}(0) = 0$ since $T_{0q} = 0$ for $q = 0$, which is also exact as for an infinite body, after an infinite time the originally localized temperature profile at the surface of the solid will give vanishing temperature increase everywhere in the solid. Energy conservation requires that

$$\int_0^\infty {\rm d}z\ T_0(z,t) = \lim_{q\to 0} \frac{T_{{\rm N}q}(t)}{2q}$$

is time independent. From (A9) we get $T_{{\rm N}q}(t) \to T_{0q}(0)$ as $q \to 0$, which is independent of time. Note that if the factor $2/\sqrt{\pi}$ would appear in (A9) then the energy conservation law would be violated.

We will now calculate $T_{0q}(t)$ using (A2):

$$T_{0q}(t) = \frac{1}{t}\int_0^t {\rm d}t'\ T_{{\rm N}q}(t')$$

Consider first the integral

$$\frac{1}{t}\int_0^t {\rm d}t'\ f(q, q_{\rm th}(t'))$$

where $q_{\rm th}(t') = 1/[4\sqrt{(Dt')}]$. Changing integration variable to $q' = 1/[4\sqrt{(Dt')}]$ we get

$$\frac{1}{t}\int_{q_{\rm th}}^\infty {\rm d}q'\ \frac{1}{8D(q')^3} f(q,q') = \int_{q_{\rm th}}^\infty {\rm d}q'\ \frac{2}{q'}\left(\frac{q_{\rm th}}{q'}\right)^2 f(q,q')$$

where $q_{\rm th} = q_{\rm th}(t) = 1/[4\sqrt{(Dt)}]$. Writing $q' = q_{\rm th}\xi$ this integral can be written as

$$\int_1^\infty {\rm d}\xi\ \frac{2}{\xi^3} f(q, q_{\rm th}\xi)$$

If we apply this result to the first term in (A8) it becomes

$$\int_1^\infty {\rm d}\xi\ \frac{2}{\xi^3}\left(1 - {\rm e}^{-q/(q_{\rm th}\xi)}\right) T_{0,q_{\rm th}\xi}(0)$$

Similarly the last term in (A8) becomes

$$\int_1^\infty {\rm d}\xi\ \frac{2}{\xi^3}\frac{q}{q + q_{\rm th}\xi} T_{0,q+q_{\rm th}\xi}(0)$$

The middle term in (A8) is time independent and unchanged. Thus we obtain from (A8):

$$T_{0q}(t) \approx \int_1^\infty {\rm d}\xi\ \frac{2}{\xi^3}\left(1 - {\rm e}^{-q/(q_{\rm th}\xi)}\right) T_{0,q_{\rm th}\xi}(0) + T_{0q}(0) - \int_1^\infty {\rm d}\xi\ \frac{2}{\xi^3}\frac{q}{q + q_{\rm th}\xi} T_{0,q+q_{\rm th}\xi}(0) \tag{A10}$$

Note that when $q_{\rm th}/q << 1$ we can expand

$$\int_1^\infty {\rm d}\xi\ \frac{2}{\xi^3}\frac{q}{q + q_{\rm th}\xi} T_{0,q+q_{\rm th}\xi}(0) \approx \int_1^\infty {\rm d}\xi\ \frac{2}{\xi^3}\left(1 - \frac{q_{\rm th}\xi}{q}\right)\left(T_{0q} + \frac{q_{\rm th}\xi}{q}\frac{{\rm d}T_{0q}}{{\rm d}q}\right) \approx T_{0q} - 2\frac{q_{\rm th}}{q}\left(T_{0q} - q\frac{{\rm d}T_{0q}}{{\rm d}q}\right)$$

When $q_{\rm th}/q >> 1$ we get

$$T_{0q}(t) \approx 2q\int_1^\infty {\rm d}\xi\ \frac{1}{\xi^4}\frac{1}{q_{\rm th}} T_{0,q_{\rm th}\xi}(0) + T_{0q}(0) - 2q\int_1^\infty {\rm d}\xi\ \frac{1}{\xi^4}\frac{1}{q_{\rm th}} T_{0,q_{\rm th}\xi}(0) = T_{0q}(0)$$

so $T_{0q}(t)$ is time independent reflecting energy conservation. In (A10)

$$T_{0q}(0) = Q\int_0^\infty {\rm d}p\ f(p,t)M(p,q) + Qf(t)N(q)$$

and the temperature in the macroasperity contact regions:

$$T_q = T_{0{\rm R}} + T_{0q}(t) + \int_0^\infty {\rm d}p\ f(p,t)M(p,q) + f(t)N(q) \tag{A11}$$

In this equation

$$f = \frac{2\mu_{\rm cont}\sigma_0 v}{\rho C_p}\frac{A_0}{A_m} - \frac{2\alpha}{\rho C_p}(T_{\rm R} - T_{\rm S}) = f_0 - \epsilon(T_{\rm R} - T_{\rm S}) \tag{A12}$$

The rubber surface temperature in the macroasperity contact regions is given by (A11) for $q = q_a$:

$$\begin{aligned} T_{\rm R} &= T_{0{\rm R}} + \int_1^\infty {\rm d}\xi\ \frac{2}{\xi^3} T_{0,q_{\rm th}\xi}(0) + \int_0^\infty {\rm d}p\ f(p,t)M(p,q_a) \\ &\quad + f(t)N(q_a) = T_{0{\rm R}} + \int_1^\infty {\rm d}\xi\ \frac{2}{\xi^3} \\ &\quad \times\left[Q\int_0^\infty {\rm d}p\ f(p,t)M(p,q_{\rm th}\xi) + Qf(t)N(q_{\rm th}\xi)\right] \\ &\quad + \int_0^\infty {\rm d}p\ f(p,t)M(p,q_a) + f(t)N(q_a) \\ &= T_{0{\rm R}} + \int_0^\infty {\rm d}p\ f(p,t) \\ &\quad \times\left[Q\int_1^\infty {\rm d}\xi\ \frac{2}{\xi^3} M(p,q_{\rm th}\xi) + M(p,q_a)\right] \\ &\quad + f(t)\left[Q\int_1^\infty {\rm d}\xi\ \frac{2}{\xi^3} N(q_{\rm th}\xi) + N(q_a)\right] \end{aligned} \tag{A13}$$

If we write this equation as

$$T_{\rm R} = T_{0{\rm R}} + \Delta T_{\rm visc} + fS,$$

we get using (A12):

$$T_{\rm R} = T_{0{\rm R}} + \Delta T_{\rm visc} + [f_0 - \epsilon(T_{\rm R} - T_{\rm S})]S,$$

or

$$T_{\rm R} = \frac{T_{0{\rm R}} + \Delta T_{\rm visc} + \Delta T_{\rm con} + \gamma T_{\rm S}}{1 + \gamma},$$

where

$$\gamma = \epsilon S = \frac{2\alpha}{\rho C_p}\left[Q\int_1^\infty {\rm d}\xi\ \frac{2}{\xi^3} N(q_{\rm th}\xi) + N(q_a)\right],$$

$$\Delta T_{\rm con} = f_0 S = \frac{2\mu_{\rm cont}\sigma_0 v}{\rho C_p}\frac{A_0}{A_m} \times\left[Q\int_1^\infty {\rm d}\xi\ \frac{2}{\xi^3} N(q_{\rm th}\xi) + N(q_a)\right],$$

and

$$\Delta T_{\rm visc} = \int_0^\infty {\rm d}p\ f(p,t) \times \left[Q \int_1^\infty {\rm d}\xi\ \frac{2}{\xi^3} M(p, q_{\rm th}\xi) + M(p, q_a) \right],$$

where

$$M(p,q) = \frac{2R}{v} \int_0^1 {\rm d}w\ \frac{q h(w)}{q + p + qp[4\pi D(2R/v)w]^{1/2}},$$

and

$$N(q) = \frac{2R}{v} \int_0^1 {\rm d}w\ \frac{q q_a h(w)}{q + q_a + q q_a [4\pi D(2R/v)w]^{1/2}}.$$

We can also write

$$\Delta T_{\rm visc} = \int_0^\infty {\rm d}p\ f(p,t) \frac{2R}{v} \times \left[\int_0^1 {\rm d}w\ \frac{q_1 h(w)}{q_1 + p + q_1 p[4\pi D(2R/v)w]^{1/2}} + Q \int_1^\infty {\rm d}\xi\ \frac{2}{\xi^3} \times \int_0^1 {\rm d}w\ \frac{q_{\rm th}\xi h(w)}{q_{\rm th}\xi + p + q_{\rm th}\xi p[4\pi D(2R/v)w]^{1/2}} \right], \tag{A14}$$

$$\Delta T_{\rm cont} = \frac{2\mu_{\rm cont}(t)\sigma_0 v}{\rho C_p} \frac{A_0}{A_m} \frac{2R}{v} \times \left[\int_0^1 {\rm d}w\ \frac{q_a h(w)}{2 + q_a[4\pi D(2R/v)w]^{1/2}} + Q \int_1^\infty {\rm d}\xi\ \frac{2}{\xi^3} \times \int_0^1 {\rm d}w\ \frac{q_a q_{\rm th}\xi h(w)}{q_a + q_{\rm th}\xi + q_a q_{\rm th}\xi [4\pi D(2R/v)w]^{1/2}} \right], \tag{A15}$$

and

$$\gamma = \frac{2\alpha}{\rho C_p} \frac{2R}{v} \left[\int_0^1 {\rm d}w\ \frac{q_a h(w)}{2 + q_a[4\pi D(2R/v)w]^{1/2}} + Q \int_1^\infty {\rm d}\xi\ \frac{2}{\xi^3} \times \int_0^1 {\rm d}w\ \frac{q_a q_{\rm th}\xi h(w)}{q_a + q_{\rm th}\xi + q_a q_{\rm th}\xi [4\pi D(2R/v)w]^{1/2}} \right]. \tag{A16}$$

References

[1] Jaeger J C 1942 *J. Proc. R. Soc. New South Wales* **76** 203
[2] Archard J F 1959 *Wear* **2** 438
[3] Holm R 1948 *J. Appl. Phys.* **19** 361
[4] Block H 1963 *Wear* **6** 483
[5] Bansal D G and Streato J L 2012 *Wear* **278–9** 18
[6] Putignano C, Le Rouzic J, Reddyhoff T, Carbone G and Dini D 2014 *Proc. Inst. Mech. Eng. Part J: J. Eng. Tribol.* **228** 1112
[7] Liu Y and Barber J R 2014 Transient heat conduction between rough sliding surfaces *Tribol. Lett.* **55** 23
[8] Persson B N J 2006 *J. Phys.: Condens. Matter* **18** 7789
[9] Persson B N J 2014 *Tribol. Lett.* **56** 77
[10] Lang A and Klüppel M 2014 *KHK 11th Fall Rubber Colloquium (Hannover, Germany, 26–28 November 2014)*
[11] Rowe K G, Bennet A I, Krick B A and Sawyer W G 2013 *Tribol. Int.* **62** 208
[12] Persson B N J, Lorenz B and Volokitin A I 2010 *Eur. Phys. J.* E **31** 3
[13] Persson B N J, Volokitin A I and Ueba H 2011 *J. Phys.: Condens. Matter* **23** 045009
[14] Persson B N J 2014 *J. Phys.: Condens. Matter* **26** 015009
[15] Barber J R 2003 *Proc. R. Soc. London* A **459** 53
[16] Greenwood J A 1966 *Br. J. Appl. Phys.* **17** 1621
[17] Campana C, Persson B N J and Müser M H 2011 *J. Phys.: Condens. Matter* **23** 085001
[18] Pastewka L, Prodanov N, Lorenz B, Müser M H, Robbins M O and Persson B N J 2013 *Phys. Rev.* E **87** 062809
[19] Persson B N J 2000 *Sliding Friction: Physical Principles and Applications* 2nd edn (Berlin: Springer)
[20] Persson B N J 2001 *J. Chem. Phys.* **115** 3840
[21] Almqvist A, Campana C, Prodanov N and Persson B N J 2011 *J. Mech. Phys. Solids* **59** 2355
[22] Scaraggi M and Persson B N J 2015 *J. Phys.: Condens. Matter* **27** 105102
[23] Lorenz B, Oh Y R, Nam S K, Jeon S H and Persson B N J unpublished
[24] Lorenz B and Persson B N J unpublished
[25] Schallamach A 1963 *Wear* **6** 375
[26] Persson B N J and Volokitin A I 2006 *Eur. Phys. J.* E **21** 69–80
[27] Persson B N J 1995 *Phys. Rev.* B **51** 13568
[28] www.tribology-abc.com/abc/history.htm